

High-resolution record of Paleoclimate during the late Quaternary, recovered from Con Moong cave - North Vietnam

Luu Thi Phuong Lan^{1*}, Brooks B. Ellwood², Nguyen Khac Su³, Wei-Hsung Wang⁴, Doan Dinh Lam⁵, Nguyen Thanh Dung¹, Nguyen Thi Mai¹

¹*Institute of Geophysics, VAST, 18 Hoang Quoc Viet, Hanoi, Vietnam*

²*Department of Geology and Geophysics, Louisiana State University, Baton Rouge, LA 70803 USA*

³*Institute of Archaeology, 61, Phan Chu Trinh, Hanoi, Vietnam*

⁴*Center for Energy Studies, Louisiana State University, Baton Rouge LA 70803 USA*

⁵*Institute of Geological Sciences, VAST, 84 Chua Lang, Hanoi, Vietnam*

Received 27 December 2022; Received in revised form 29 May 2023; Accepted 24 July 2023

ABSTRACT

To clarify the paleoclimatic events in Northern Vietnam during the Late Quaternary, 132 Con Moong - Thanh Hoa cave sediment samples were collected to analyze magnetic susceptibility (χ), $\delta^{18}\text{O}$, and $\delta^{13}\text{C}$. Based on the tendency in the value of χ Con Moong's sediment, 14 climate zones that change continuously from warm to cold were identified. These climate zones also correspond to the changing trend of $\delta^{18}\text{O}$ and $\delta^{13}\text{C}$. The period of 14 magnetic zones is referenced from the extrapolation of four ^{14}C dating. These alternating cold-warm χ sequences correspond to the Composite Reference Section (CRS) developed in Southern Europe from a χ zonation of multiple caves. The paleoclimate characteristics, including the Heinrich H2 and H1 climate events, the Bølling/Allerød, and Younger Dryas warm-cold events, were elucidated for Northern Viet Nam from ~28.000 to ~10.000 yr BP.

Keywords: Paleoclimate, magnetic susceptibility, stable isotopes, YD, Heinrich H1, H2.

1. Introduction

Since the Last Glaciation Maximum (LGM), several significant, short-term global climatic events are known, including the Heinrich H2 and H1, the Bølling/Allerød warm-cool cycle (Wang et al., 2001; Rasmussen et al., 2006), and Younger Dryas (YD), observed in ice cores, in sedimentary sections in North America (Canada and the United States), Europe (France, Portugal, Scotland, Spain), Japan, New Zealand, Peru, and in speleothems from China and Indonesia (Broecker, 1992; Alley et al., 1997; Herz and

Garrison, 1998; Wang et al., 2001; Harrold et al., 2004; Hemming, 2004; McManus et al., 2004; Rohling and Pälike, 2005; Keigwin et al., 2005; Ellwood and Gose, 2006; Walker et al. 2008 and 2009; Wu et al., 2009; Griffiths et al., 2010; Ballantyne, 2012; Schmidt et al., 2012; Ma et al., 2012; Rohling et al., 2009; Thompson et al., 1995; Heinrich H., 1988). These paleoclimatic events could be identified in Con Moong Cave, Thanh Hoa Province, Northern Vietnam. Probably the most important of these post-LGM events is the YD Stade, which represents a time when the trend toward global climate warming was interrupted following the LGM.

*Corresponding author, Email: luuphuonglan@gmail.com

During the prehistoric period, people living in Northern Vietnam were often forced to live in caves due to the high precipitation and cold temperatures known to have periodically existed in the SE Asian region (Griffiths et al., 2010, Anderson, 1997; Barker et al., 2005; Morley & Goldberg, 2017; O'Connor et al., 2017; Wurster & Bird, 2016). Con Moong Cave (Fig. 1) is important because of its

imposing cultural and human remains. Furthermore, this cave is located in the Cuc Phuong National Park (20°40'86.0"N, 105°65'16.4"E), as well as the significant accumulations of snail shells and hundreds of tools made from pebbles, bone, horn and shell material that represent a sequence from Proto-Hoabinhian to Hoabinhian archaeological cultures in the region.



Figure 1. (a) Location map of Con Moong Cave in Thanh Hoa Province, Vietnam; (b) the karst location in Vietnam; (c) Section sampled for this paper

There are many approaches to studying Paleoclimate. And studying paleoclimates through such proxies as the magnetic

susceptibility ($MS-\chi$), stable isotope ($\delta^{18}O$, $\delta^{13}C$), is one of them. Climate controls the magnetic properties of sediments deposited in

caves. This sediment was originally formed outside the cave. They are subjected to alternating oxidation and reduction processes that produce magnetic minerals, mainly maghemite, and magnetite, which dominate the magnetic susceptibility (χ of these sediments). This material is then eroded, washed, blown, or tracked into and deposited within caves, with the resulting sediment stratigraphy providing samples for dating χ and stable isotope measurement. Within caves, where the sediments are protected, the climate record.

Previous studies applying low-field measurements to micro-stratigraphic sediment sample sets (essentially continuous samples) recovered from well-documented Pleistocene and Holocene archaeological sites in Europe and the United States have documented that χ serves well as a climate proxy that is recorded in cave sediments (e.g., Ellwood et al., 1997, 2001, 2004; Harrold et al., 2004; Ellwood and Gose, 2006). Much of this work result from the Graphic Correlation of χ versus sediments-age profiles from several caves in Southern Europe. Caves in Albania, France, Portugal, and Spain were used to build a composite reference section (CRS) for climate across Southern Europe (SE). That CRS is used here for climate comparison between Mid-Latitude SE Europe and Low-latitude Southern Asia. In recent years, some paleoclimatic and paleoenvironmental records from different archives around Southeast Asia have been published, such as lacustrine sediments in the Central Highlands of Vietnam (Huong et al., 2023). Or the $\delta^{18}\text{O}$ values of speleothems collected from Southeast Asia have been proposed to represent the paleo-precipitation change in the late Pleistocene uniquely (Nguyen et al., 2020), and the high-resolution $\delta^{18}\text{O}$ record from Thuong Thien Cave offers evidence of synchronous climate change associated with H-3 (Nguyen et al., 2022).

In conjunction with archaeological excavations, isotopic dating, and cultural associations χ can provide high-resolution

relative dates (Ellwood et al., 2001; Harrold et al., 2004). These relative dates are based on χ trends from dated, excavated stratigraphic sequences from Southern Europe to establish the regional CRS developed by graphically correlating between excavation units that overlap in age. During the last 4.000 to 50.000 years in Europe, 17.5 χ zones (cycles) were identified, and half-cycles were labeled SE-1 to SE-35. These cycles indicate relative climate fluctuations from colder to warmer periods. The 2001 SE CRS (Ellwood et al., 2001) was updated in 2004 by adjusting the dates and extending the relative time scale back to ~46.000 BP (uncalibrated; Harrold et al., 2004). Using the web-based CalPal program, calibration of this data set extends the Harrold et al. (2004) χ -based zonation back to ~50.000 BP for Southern Europe.

We present the results of multi-parameter studies: χ , stable isotopes ($\delta^{18}\text{O}$, $\delta^{13}\text{C}$), and ^{14}C -dated geology of excavated Pleistocene deposit in Con Moong cave to elucidate the late Pleistocene climate event whose stratigraphy reflects the same geological activities in the cave.

2. Sample collection and study methods

Con Moong Cave was discovered and excavated in 1976 (Thong, 1980), but until 2008 the exploration hole was repaired to a depth of 3.6 m (Su, 2009). Until 2010-2014, Vietnamese-Russian archaeologists continued to excavate from a depth of 3.6 m to 10.14 m (Su, 2014). This paper presents the study result taken at 3.3 m belongs to the 3.6 m depth of the top sequence (we don't use the upper 0.3 m sediment of the section because it is disturbed).

2.1. Magnetic susceptibility ($MS-\chi$)

132 sediment samples for χ measurement were collected in a continuous profile (~ 2 cm/1 sample) through ~ 3.3 m of the upper layers of Con Moong cave (Fig. 1c, Fig. 2). These samples were taken along the 1–17 archeological levels. These

archaeological levels are also given in Fig. 2a, as are calibrated ^{14}C dating (Table 1). Samples were sent to Louisiana State University (LSU), sieved to isolate the less than 1 mm size fraction, and carefully weighed. Sieving was

employed to remove coarse-grained elements of the sample that were not part of the climate-affected sediment, such as large fragments of calcite, bone, shell, and artificial material that might otherwise influence χ .

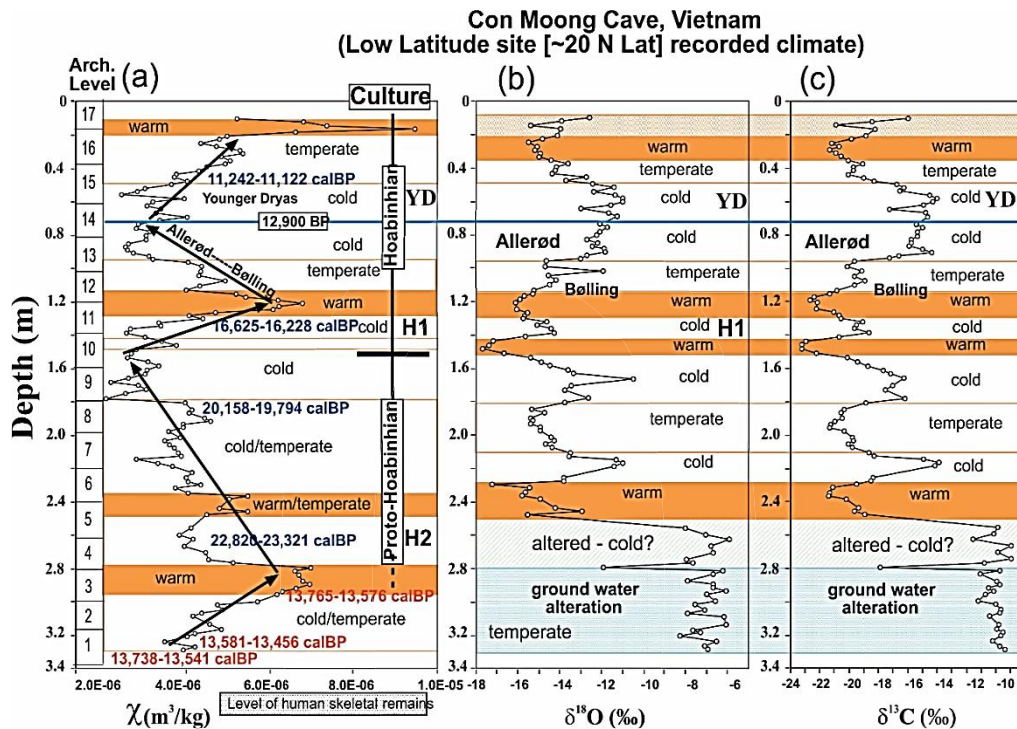


Figure 2. (a) Depth versus magnetic susceptibility (χ) for ~ 3.3 m of continuous sediment samples collected in Con Moong Cave, Vietnam, from archaeological levels 1–17 (Su, 2009). All samples contain small shell fragments. The range of Proto-Hoabinhian to Hoabinhian cultures is identified. Unaltered ^{14}C dates are shown in black. The cold climate perturbations, Heinrich H2, Heinrich H1, Allerød-Bölling, and Younger Dryas are based on observed χ cycles, where values trending toward the left indicate cooling trends, while values trending toward the right represent warming trends (arrows in Fig. 2a); (b) $\delta^{18}\text{O}$ (‰VPDB) for shell samples collected in Con Moong cave; (c) $\delta^{13}\text{C}$ (‰VPDB) for shell samples collected in Con Moong cave

Table 1. Con Moong Cave Samples ^{14}C Dates (N = 7)

Samp. ID	Lab index	Conventional data yr BP	Calibrated age (cal) 2σ age	$\delta^{13}\text{C}$ ‰	$\delta^{18}\text{O}$ ‰	Depth (m)	Dated material
CM18-19	Beta 537507	9,750 \pm 40	11,242-11,122 calBP	-25.5	n/a	0.47 m	Snail shell
CM53-54	Beta 537508	13,620 \pm 40	16,625-16,228 calBP	-24.3	n/a	1.24 m	Snail shell
CM79-80	Beta 537509	16,560 \pm 40	20,158-19,794 calBP	-20.6	n/a	1.86 m	Snail shell
CM110-111	Beta 537510	19,120 \pm 50	23,321-22,820 calBP	-24.0	n/a	2.73 m	Snail shell
CM118aa	Beta 555789	11,870 \pm 30	13,765-13,576 calBP	-8.1	-4.3	2.89 m	Skull fragments
CM131aa	Beta 547418	11,710 \pm 30	13,581-13,456 calBP	-9.2	-10.8	3.27 m	Skull fragments
CM132aa	Beta 547418	11,790 \pm 30	13,738-13,541 calBP	-9.2	-5.8	3.29 m	Skull fragments

All measurements reported in this paper were performed using the susceptibility bridge at LSU, with a sensitivity that allows

measurement samples to $1 \times 10^{-10} \text{ m}^3/\text{kg}$. The instrument is easy and fast to use, and the measurement coil is optimized for small

samples (30g or less). The bridge is calibrated using standard salts for reported values (Swartzendruber, 1992). We report M.S. regarding sample mass because measuring with high precision is much easier and faster than volume (Ellwood et al., 1988). Each sample is measured three times, and these measurements' mean and standard deviation were calculated. χ is then calculated from these measurements, and the results are plotted relative to depth (Fig. 2a).

2.2. Stable carbon and oxygen isotope analyses

Fossil snails are used for study as an archive of Paleoclimate and paleoenvironment because they are more sensitive to climatic changes than other nonbiogenic tissues. Taxonomic analyses of the snail assemblages have been extensively conducted and applied in paleoclimate reconstruction (Laurin & Rousseau, 1985; Moine et al., 2002; Wu et al., 1996; 2002; 2006; Wu & Wu, 2008; 2011), and with the development of stable isotope techniques, the carbon and oxygen isotopic compositions of snail shell carbonate ($\delta^{13}\text{C}$ shell and $\delta^{18}\text{O}$ shell) have been analyzed to determine new proxies for providing paleoenvironmental and

paleoecological information.

At LSU, 132 sediment samples from Con Moong Cave were used to extract snail shell fragments. This material is used to measure $\delta^{18}\text{O}$ and $\delta^{13}\text{C}$. Stable isotope measurement results are reported relative to the Vienna Pee Dee Belemnite (VPDB) standard. The climate influences these fragments at the time they live. As surface soils, this material is eroded, washed away, blown away, or tracked and deposited in caves to create sedimentary strata that provide samples for dating within the cave. The measurement results of the $\delta^{18}\text{O}$ sample are shown in Fig. 2b, and the $\delta^{13}\text{C}$ are shown in Fig. 2c.

2.3. ^{14}C dating

Through a 3.3 m section, seven samples were taken for ^{14}C dating (Table 1, Fig. 3). The top four samples (shown in black in Fig. 3) are snail shell fragments. They are brought into the cave from the outside with sediments, where they are affected by the climate at the time they lived. Due to the flow of silt or the footprints of humans or animals, these shell fragments were carried into the cave and accumulated in the cave.

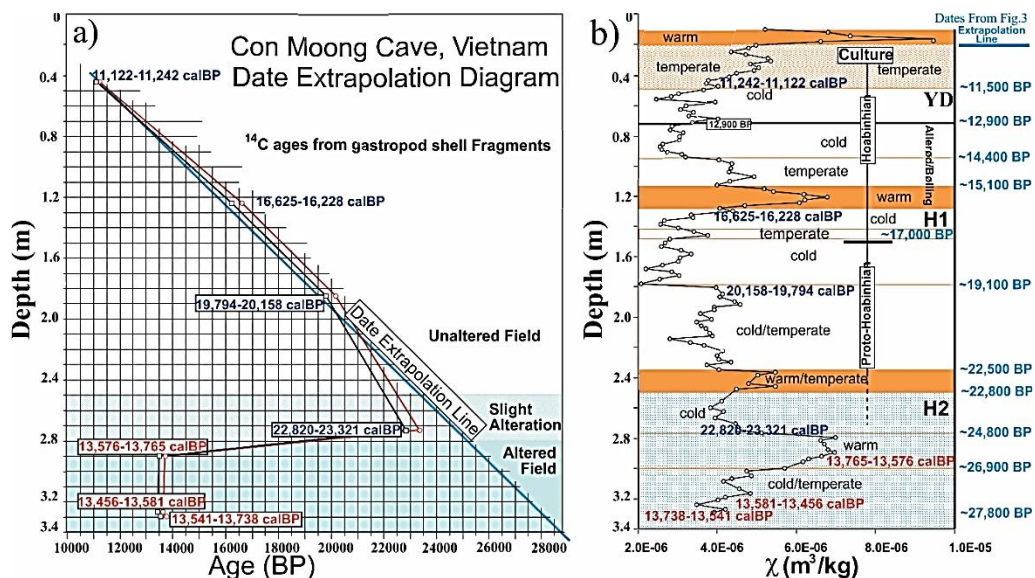


Figure 3. a) Date extrapolation for Con Moong Cave using the ^{14}C dating available from the section (Table 1). b) Extrapolated age at section

The remaining three samples below the section (shown in red, Fig. 3, Table 1) are three skull fragments from 3 sets of remains. They are dated at Beta Analytic, USA by AMS (Accelerator Mass Spectrometry) method (<https://www.radiocarbon.com/accelerator-mass-spectrometry.htm>).

3. Results

3.1. MS

The χ value fluctuates from $2.09 \times 10^{-6} \text{ m}^3/\text{kg}$ (at a depth of 1.76 m) to $9.47 \times 10^{-6} \text{ m}^3/\text{kg}$ (at a depth of 0.1 m). They fluctuate around $4.0 \times 10^{-6} \text{ (m}^3/\text{kg)}$. The cold climate perturbations are based on observed χ cycles, where values trending toward the left indicate cooling trends while values trending toward the right represent warming trends (arrows in Fig. 2a). From top to bottom of the section, based on the tendency of the MS results, they are divided into 14 MS zones (discussed in Section 3.5 below): 1. Warm, 2. Temperate, 3. Cold, 4. Cold, 5. Temperate, 6. Warm, 7. Cold, 8. Temperate, 9. Cold, 10. Cold/temperate, 11. Warm/temperate, 12. Cold/temperate, 13. Warm, 14. Cold/temperate (Fig. 2a).

3.2. Stable carbon and oxygen isotope analyses

The $\delta^{13}\text{C}$ values are in the range of -23.27 at a depth of 1.48 m to -9.57‰ PDB at a depth of 2.67 m, and the ranges of $\delta^{18}\text{O}$ values are -17.73 at a depth of 1.48 m to -5.7‰ PDB at a depth of 2.63 m. The results for both the $\delta^{18}\text{O}$ (Fig. 2b) and the $\delta^{13}\text{C}$ (Fig. 2c) values abruptly change to much heavier values above ~2.5 m depth in the section, with a mean $\delta^{18}\text{O}$ and $\delta^{13}\text{C}$ values of -13.97‰ PDB and -8.89‰ PDB, respectively. The $\delta^{18}\text{O}$ values range from -17.73‰ to -10.38‰ PDB, and the $\delta^{13}\text{C}$ values are from -23.27 to -14.32‰ PDB. In contrast, the $\delta^{18}\text{O}$ and $\delta^{13}\text{C}$ values show tiny variations below ~2.5 m depth in the section, with a mean of -7.06‰ PDB and -4‰ PDB,

respectively. The $\delta^{18}\text{O}$ and $\delta^{13}\text{C}$ show from -7.88‰ to -6.81‰ PDB and -18.17‰ to -9.7‰ for in the below of 2.5 m), respectively. The tendency of the $\delta^{18}\text{O}$ (Fig. 2b) and the $\delta^{13}\text{C}$ (Fig. 2c) are divided into zones equivalence with MS zones: 1. Warm, 2. temperate, 3. cold, 4. cold, 5. temperate, 6. warm, 7. cold, 8. temperate, 9. cold, 10. temperate, 11. cold/temperate, 12. Warm (Fig. 2b, c) from top to bottom of the section.

3.3. ^{14}C dating

The results show in (Table 1). Date extrapolation for Con Moong Cave using the ^{14}C dates available from the section (four upper samples in Table 1). From ~0.4 m to ~1.87 m (~ 11.200 to ~ 20.000 calyr BP), the dates with depth are linear, with a line of extrapolation beginning to depart from a linear trend at ~2.7 m depth (at ~ 23.000 calyr BP), to what is slight alteration within the lower part of the section. Below ~2.7 m depth (before ~23.000 calyr BP), three ^{14}C dating from 2.9 to 3.3 m overlap in age and are anomalous due to groundwater alteration in the section below 2.5 m depth (Fig. 2), occurring at ~ 13.500 calyr BP (Table 1). These three dating ^{14}C deviate from the linear trend.

4. Discussions

4.1. General considerations

The strict definition of Heinrich events is the climatic event causing the Ice Rafted Debris (IRD) layer observed in marine sediment cores from the North Atlantic: a massive collapse of northern hemisphere ice shelves and the consequent release of a prodigious volume of icebergs. By extension, the name "Heinrich event" can also refer to the associated climatic anomalies registered at

other places around the globe, at approximately the same periods. The layers are generally considered to fall within six brief intervals during the last glacial period, labeled "H1" through "H6" from youngest to oldest. The events are thought to have peaked at about 16,800 (H1), 24,000 (H2), 31,000 (H3), 38,000 (H4), 45,000 (H5), and 60,000 (H6) years ago (Hemming, 2004).

Some researchers identify the Younger Dryas event as a Heinrich event, making it an event H0 (Broecker, 1994). Younger Dryas is essential in archaeology, given that it is clear that at higher latitudes, at ~13,000 BP, the effect of Younger Dryas cold intensification appears to have resulted in the post -13,000 year disappearance of Clovis Cultures in North America (PIDBA; <http://pidba.utk.edu>).

The back-to-back (continuous) sampling of sediments collected from Con Moong Cave, Viet Nam, yielded χ , $\delta^{18}\text{O}$, and $\delta^{13}\text{C}$ data, along with new ^{14}C dating, which demonstrate that multiple climatic events have been recorded in the ~3.3 m section sampled in the cave (Fig. 2). Coherent trends exist in the data sets from Con Moong Cave, and these are supported by multiple samples. These trends are clearly not chaotic. The overall trends in χ , $\delta^{18}\text{O}$, and $\delta^{13}\text{C}$ (Fig. 2), show no large or abrupt changes above 2.5 m (after ~22,000 yr BP) in the section. Furthermore, the new ^{14}C dating χ , $\delta^{18}\text{O}$, and $\delta^{13}\text{C}$ data sets (Fig. 2), are interpreted here as exhibiting trends that indicate warm to cold climatic effects in the section above 2.5 m (after ~22,000 yr BP). These trends are consistent with known climatic variations from 28,000 to ~10,000 yr BP interval recovered from analysis of stalagmites from Hulu Cave in China (Wang et al., 2001). The χ , $\delta^{18}\text{O}$, and $\delta^{13}\text{C}$ data from Con Moong Cave show essentially the same climate trends (Fig. 2). Still, before ~22,000 yr BP (below ~2.5 m depth) in the Con Moong Cave sequence, there are

alteration effects on the $\delta^{18}\text{O}$ and $\delta^{13}\text{C}$ data sets (Fig. 2b and c), interpreted as due to acidic ground water penetration into the sampled interval at that depth. However, the χ trends are not altered in the way that the $\delta^{18}\text{O}$ and $\delta^{13}\text{C}$ data sets are altered, and therefore the χ data are interpreted here as reflecting climatic variations back to ~28,000 yr BP.

4.2. Testing χ stability in cave samples

The question concerning the stability of χ values in cave sediments is addressed here by showing results from Cova Beneito, Spain, where the sediments have been altered. Figure 4a presents the χ data from a section covering 3 m of Cova Beneito, through which samples for χ measurement were collected and analyzed. The identical methods were used on samples from Cova Beneito, as in Con Moong Cave. The χ pattern for Cova Beneito shows typical, unaltered values χ above the ~4.5 m level, where magnetite and maghemite dominate. Still, below 4.5 m, the sediments in the cave were altered due to groundwater effects (Fig. 4a). This resulted in the alteration of the primary iron mineralogy and the production of secondary goethite in the section below 4.5 m. Below this level, values χ in the section precipitously dropped by an order of magnitude, and the lower part of the section was discolored yellow due to diagenesis in the section to the iron mineral goethite (FeOOH). None of the alteration effects observed in Cova Beneito Cave are observed in the Con Moong Cave χ results (Figs. 2 and 4). Given are the sample numbers and χ range measured for the samples before heating (Fig. 4b). 2 samples were chosen from the unaltered samples and 2 from altered samples #25 and #27 (Fig. 4b); alteration was due to ground water migration through samples #80 and #85 (Fig. 4b) and the production of goethite while destroying magnetite and maghemite, present in the samples before alteration.

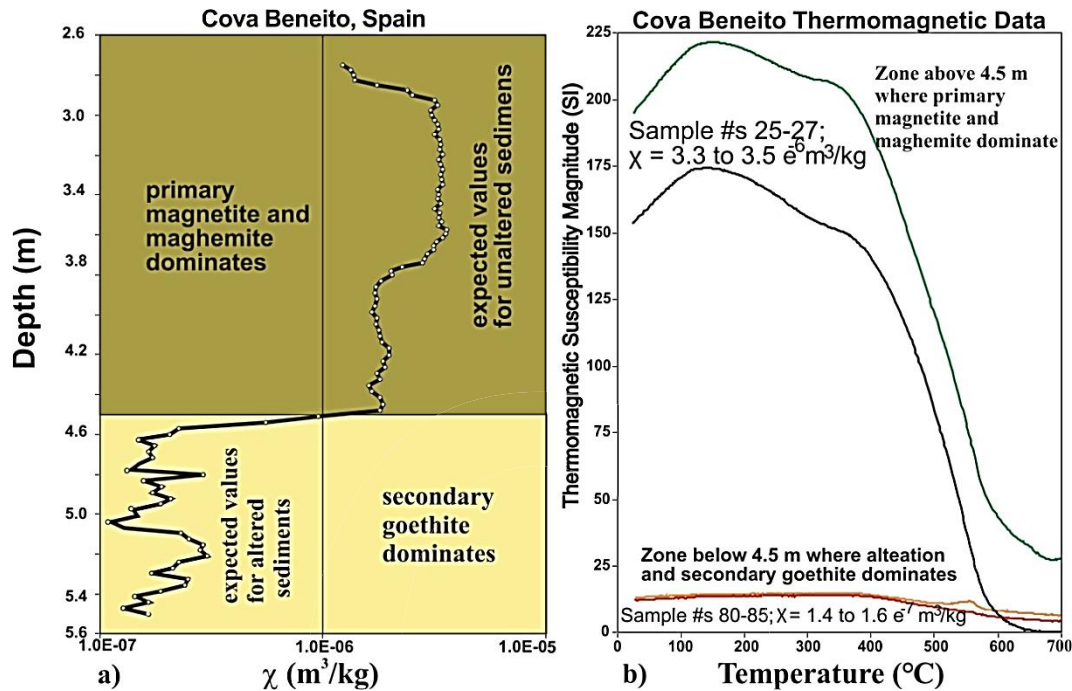


Figure 4. a) χ measured for samples from Cova (cave) Beneito, Spain, where typical alteration effects occur, with brown at the top representing unaltered samples that χ arises from magnetite and maghemite; and yellow below-representing alteration of the iron mineralogy to goethite, where an order of magnitude decrease in χ is observed; b) Thermomagnetic susceptibility magnitude (κ in SI) heating curves for 4 samples from the Cova Beneito section reported here

4.3. Problems ^{14}C dating, $\delta^{13}\text{C}$, and $\delta^{18}\text{O}$ data: acidic, deep, ground water alteration effects below 2.5 m depth in the sampled sequence

^{14}C dating of Con Moong cave is graphically reported in Fig. 3 and Table 1. Beginning at $\sim 2.5\text{-}2.7$ m depth in the Con Moong measured section, the ^{14}C dating for Con Moong cave deviates from a linear age trend. In addition, at ~ 2.5 m in section, there is a primary ~ 9 to 11% significant shift in both $\delta^{13}\text{C}$ and $\delta^{18}\text{O}$ toward heavier values (Fig. 2b and 2c), and slight variation is observed in ^{14}C , $\delta^{13}\text{C}$, and $\delta^{18}\text{O}$ for the rest of the section sampled, ~ 0.5 m of section. These changes are attributed to acidic groundwater penetration at $\sim 13,500$ yr BP (based on three ^{14}C dating from ~ 2.9 to 3.3 m within the measured section; Fig. 3; Table 1). The

proposed acidic alteration process is discussed above in Section 2.3, but the upper part of the section, above ~ 2.5 m, was not altered. Note that the χ data do not appear to have been altered in the section (Fig. 2a).

4.4. ^{14}C analysis of human bones from burials (3 skeletons) at ~ 3.6 m depth in the measured section

Notably, the three lowest dates within the section, below 2.5 m, are identical at $\sim 13,500$ calyr BP (Table 1), and deviate significantly from the linear date extrapolation line of ^{14}C dating in Fig. 3. The interval below 2.5 m depth also contains the anomalous $\delta^{13}\text{C}$ and $\delta^{18}\text{O}$ data (Fig. 2b and 2c) the age of shells was determined by ^{14}C dating method (Table 1), and we argue that the acidic ground water penetration through the section at $\sim 13,500$ yr BP replaced the calcite in the

shells measured, with younger ^{14}C in the shell CaCO_3 . At the same time, this process destroyed the bone collagen. Therefore, it was impossible to date any of the bone fragments sent for dating to Beta Analytic, who reported that the bone collagen was destroyed and not replaced. The alteration effects reported here were below the 2.5 m level, and therefore, the penetrating acidic groundwater must have come in laterally or flowed up from below the section. It did not percolate down through the section from the top, or all the dates would have been 13.500 yr BP. The bones may have been much older but can't be dated using the ^{14}C dating method.

4.5. Climate events

14 alternating cold-warm χ sequences (14 MS zones) observed in Con Moong Cave have been correlated to the Composite Reference Section (CRS). This CRS developed in Southern Europe from a χ zonation recovered from multiple caves in Albania, France, Portugal, and Spain. In these sections, both continuous χ measurement and ^{14}C ages were used in building the Southern European SE-CRS reported by Harrold et al. (2004). The Ages of 14 magnetic regions are referenced from the extrapolation of 4 ^{14}C dating (Fig. 3a). According to this reference, within the studied section, the events with the corresponding ages indicated in the right margin of Fig. 3b (in blue) are The Heinrich H2 climate perturbation: from ~24.800 to ~22.800 yr BP; The Pre-Heinrich H1 climate perturbation: from ~18.800 to ~17.500 yr BP; The Heinrich H1 climate perturbation: from ~17.500 to ~16.500 yr BP; The Bølling-Allerød climate cycle sets: from ~16.500 to ~12.900 yr BP (see more in 3.5.3 below); Younger Dryas: from ~12.900 to ~11.500 yr BP; these zonations are also correlated to Hulu Cave in China (Wang et al., 2001) in Fig. 5. A segment of the European CRS is shown here along the right margin in Fig. 5,

where the dates from Harrold et al. (2004) are calibrated using the CalPal web-based program. The climatic events recorded by χ data from within Con Moong Cave (Fig. 2a), are interpreted to represent ~18.000 years, from ~28.000 to <10.000 yr BP, covering the SE-CRS interval from SE24 to SE13 (Fig. 5b). In Con Moong Cave, a Southern Asia (SA) time scale is used to denote the equivalent cold-warm intervals that correspond to those zones in southern Europe and eastern China.

4.5.1. The Heinrich H2 climate perturbation

Toward the base of the measured section, beginning at ~2.5 m in the section, at the base of archaeological Level 4 and including most of Level 5, is the Heinrich H2 cold/temperate χ low zone (Fig. 5b). H2 begins at ~24.800 calyr BP and extends to ~22.800 calyr BP represents ~2.000 years of deposition within Con Moong Cave. This duration and time coincide with the results from Hulu Cave, China (Wang et al., 2001) (Fig. 5).

4.5.2. The Pre-Heinrich H1 climate perturbation

The Heinrich H1 cycle/event was preceded by a long-term cooling trend that began in archaeological Level 9 and extended into Level 11, the H1 event (Fig. 5b), and is correlated to the beginning of the SE-20 cold event in Europe (Fig. 5c). This extends through a temperate zone (SE-20, Fig. 5c), that ends in the H1 cold event. This European cold event lasted for ~1.300 years (data from Harrold et al., 2004) that was corrected using the WEB-based CalPal program.

4.5.3. The Heinrich H1 climate perturbation

Heinrich events were first identified based on the observation of ice-rafted debris concentrations in North Atlantic piston cores (Heinrich, 1988; Hemming, 2004), and shown to be followed immediately by an abrupt

warming event (Thompson et al., 1995). The mechanism for driving the massive iceberg fluxes into the North Atlantic is not known, but the timing of H1 Heinrich event/cycle begins with a cold cycle followed immediately by an abrupt warming. In Con Moong Cave, the H1 cold event begins in archaeological Level 10 at ~17.500 yr BP and ends in Level 11 at ~16.500 yr BP. The corresponding warm event extends from Level 11 and into Level 12 (Figs. 2a & 3b) The H1 cycle/event has also been identified in Halls Cave, Texas (Ellwood and Gose, 2006), but there, the second part of the H1 cycle exhibits an intense and abrupt warming peak, while the initial cold is muted. Timing is approximately the same as the H1 event in Vietnam, given the uncertainties inherent in the ^{14}C dating method.

4.5.4. The Bølling-Allerød Climate Cycle Sets

In Con Moong Cave deposits, between the end of the Heinrich H1 event, at ~16.500 yr BP, and the beginning of Younger Dryas at ~12.900 yr BP, there is recorded a ~3.500 year-long double cycle, progressively getting cooler through time, that we interpret here to be the Bølling/Allerød cycle interval. The earliest of these cycles is also identified in the Hulu Cave data set in eastern China and labeled as Bølling-Allerød. Still, the second cycle is not explicitly labeled but is included by Wang et al. (2001). Because of the expanded nature of the Con Moong Cave section, there are two cycle sets that we are labeling here collectively as the Bølling-Allerød cycles. These cycles represent a clear trend identified in Figs. 2a and 5a as the Bølling-Allerød trend.

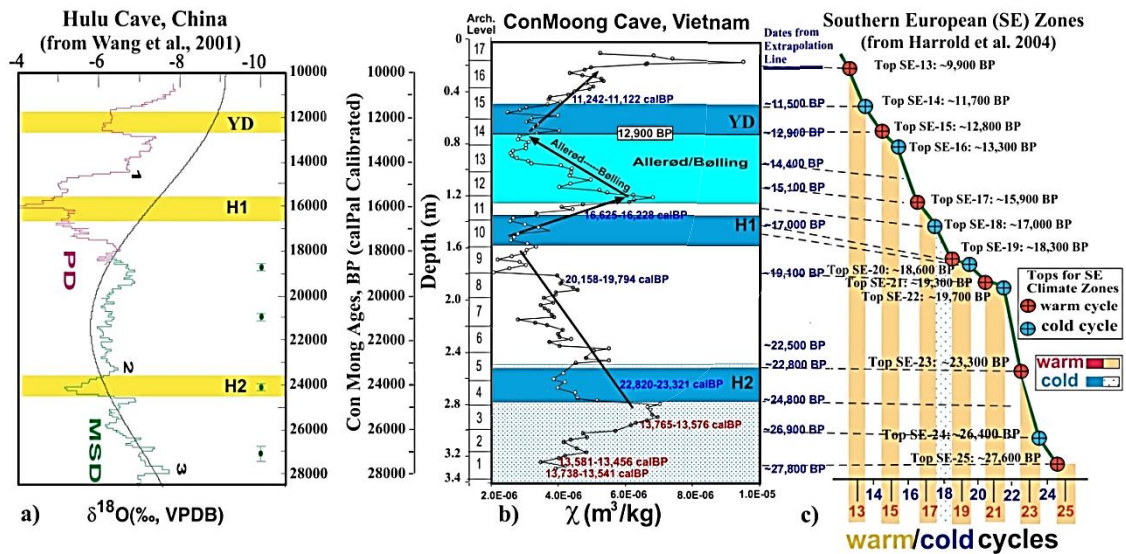


Figure 5. Graphic comparison, dashed lines, of magnetic susceptibility data from Con Moong Cave (Fig. 2a) to an updated climate cyclicality from the Harrold et al. (2004) time-scale for Southern Europe (SE). (a) Event climate from Hulu cave, China; (b) Ages in Con Moong sediments in black along the left of the diagram are extrapolated from the reliable ^{14}C calyr BP dates in Table 1, with date extrapolation from Fig. 3; ages in Blue along the right side of the diagram were given in Fig. 3b; ages in Red are from within the zone of alteration in Con Moong Cave identified in Fig. 2 and Fig. 3a, and given in Table 1. Cold-warm climate variability from Fig. 2; (c) The Harrold et al. (2004) uniform SE cold-warm cyclicality is labeled along the lower (x)-axis, and date ranges are given along the right margin of the Harrold et al. (2004) SE climate curve

4.5.5. *The Younger Dryas climate event*

It is well known that global climate at a given time is manifested differently from place to place on the Earth, so in Vietnam, a climate event may last longer or be shorter relative to its global location. For example, in Southern Europe, while the Younger Dryas event lasted for ~1.200 years, from ~12.800 to ~11.600 yr BP (Harrold et al., 2004; Fig. 5b), in Vietnam, Younger Dryas is recorded in Con Moong Cave to have lasted for ~1,400 years (Fig. 5a), from ~12.900 to ~11.500 yr BP. However, the global range for Younger Dryas has been established from ~12.900 to ~11.700 yr BP by international agreement (Walker et al., 2008). At Hulu Cave in eastern China, Younger Dryas is reported as having occurred from ~12.800 to ~11.500 yr BP (Wang et al., 2001), essentially identical to ages from Con Moong Cave, Vietnam. The $\delta^{18}\text{O}$ and $\delta^{13}\text{C}$ data sets also reflect this age range for Younger Dryas in Con Moong Cave and within Hulu Cave stalagmites (Wang et al., 2001).

4.6. *Climate comparisons between Eastern Asia (Vietnam and China) and Southern Europe*

Given that the significant climate trends, from H2 to YD exhibited in the Con Moong Cave data set, are global features, the time scale published by Harrold et al. (2004) for Southern Europe provides a template to which the Con Moong Cave data set can be compared (Fig. 5). In Fig. 5, calibrated ages from the SE-CRS of Harrold et al. (2004) are graphically compared to the Con Moong Cave section. The purpose of Fig. 5 is to visually show the correspondence between the timing and climate trends exhibited between the European climate zonation and the Con Moong Cave succession. The dates presented in Fig. 5 are approximately the same between the two locations (Europe and Vietnam). Presented in Fig. 5 is a uniform SE zonation

compared with a uniform time scale for the period from 28.000 to 10.000 yr BP, and includes the last significant global ice fields (LGM). Towards the end of the LGM in the Harrold et al. (2004) data set, there is a slight compression of the data in Southern Europe through the end of the LGM (SE-22 to SE-19), at the end of which the Heinrich H1 cycle begins. In Europe and in Vietnam, H1 begins with the cold SE-18 event, and then an abrupt warming, the beginning of the Bølling-Allerød cycle, occurs, represented by SE-17 in Europe. In Europe and Vietnam, the H1 cycle lasts for ~1.000 years (Fig. 5). The last comparable sediment sequence in Con Moong Cave is warm event SE-13, which appears to be an abrupt warming that may be truncated at the top. Still, the ages are generally consistent between the Vietnamese and European data sets - given the dating uncertainties. The date sequencing for the Vietnamese data presented here also compare well with the Hulu Cave stalagmite data from China (Wang, et al., 2001).

Measured in sediment collected from Archaeological Levels 1 and 2 (Fig. 5) are temperate χ values representing the interval between Heinrich H3 and H2 events. Immediately following that, at ~25.800 yr BP is a warm event that is mainly captured in Level 3, and immediately following that is the cold/temperate H2 event, recovered mainly from Levels 4 and 5. Using the SE-23 CRS ages for this interval, the H2 cooling occurs at Con Moong Cave from ~24.800 to ~22.800 yr BP.

The next distinctive climate event in the Con Moong sequence is the Heinrich H1 cycle found mainly in Level 11, at ~1.35 m in the section, with a date range from ~17.200 to ~16.500 yr BP. This is followed by the ~3.000 years Bølling-Allerød cooling trend in Vietnam (Fig. 5a), followed by the YD Cold Stade covers ~0.2 m of the section sampled in the cave. From archaeological Levels 5 through Level 16, both the $\delta^{18}\text{O}$ and $\delta^{13}\text{C}$ data

sets show the same climate events/trends as the χ data set (Fig. 2b and 2c). However, the H1 cycle in the SE data set overlaps a bit but is slightly older than observed in Vietnam, with the cold SE-8 representing the H1 part of this climate trend, ranging from ~18.300 to ~17.000 yr BP (Harrold et al., 2004). A better correlation is observed between the data set in Halls Cave, Texas, where H1 dates are comparable, but the event in Texas was warm (Ellwood and Gose, 2006).

5. Conclusions

The Con Moong Cave's magnetic susceptibility (χ) data set reported herein, is compared with similar χ results from Southern Europe and Eastern China and covers an age range from ~28.000 yr BP to <10.000 yr BP captured for sedimentary deposits from the Con Moong Cave, Vietnam. The following climatic events are identified: (a) Heinrich H2 within Levels 4 and 5, at ~24.800 to 22.800 yr BP; (b) the Heinrich H1, within Level 10 and ending in Level 11, at ~17.500 to ~16.500 yr BP, with the cycle ending in an abrupt warming event. This is followed by two warm-cold cycles in Level 11 through the lower half of Level 14, the Bølling-Allerød climate trend containing two warm-cold cycles, from ~16.000 to ~12.900 yr BP. Next is Younger Dryas (YD) from ~12.900 to ~11.500 yr BP, in Levels 14 to 15, and the beginning of the Holocene.

Acknowledgements

Funding for the project was provided by the VietNam Academy of Science and Technology under the NVCC 12.01/22-22 grant number and by the Robey Clark endowment to Ellwood from LSU. We thank Amber Ellwood for performing technical work.

References

Alley R.B., K.M. Cuffey, E.B. Evenson, J.C. Strasser, D.E. Lawson, G.J. Larson, 1997. How glaciers

- entrain and transport basal sediment: Physical constraints. *Quaternary Sci. Rev.*, 16(9), 1017-1038. Doi: 10.1016/s0277-3791(97)00034-6.
- Anderson D.D., 1997. Cave archaeology in Southeast Asia. *Geoarchaeology*, 12(6), 607-638. [https://doi.org/10.1002/\(SICI\)1520-6548\(199709\)12:63.0.CO;2-2](https://doi.org/10.1002/(SICI)1520-6548(199709)12:63.0.CO;2-2).
- Ballantyne C.K., 2012. Chronology of glaciation and deglaciation during the Loch Lomond (Younger Dryas) Stade in the Scottish Highlands: implications of recalibrated ^{10}Be exposure ages. *Boreas*, 41, 513-526.
- Barker G., T. Reynolds, D. Gilbertson, 2005. The human use of caves in Peninsular and Island Southeast Asia: Research themes. *Asian Perspectives*, 44(1), 1-15. <https://doi.org/10.1353/asi.2005.0003>.
- Broecker W.S., 1992. Defining the boundaries of the late-glacial isotope episodes. *Quaternary Res.*, 38, 135-138.
- Dung Chi Nguyen, et al., 2020. A decadal-resolution stalagmite record of strong Asian summer monsoon from northwestern Vietnam over the Dansgaard-Oeschger events 2-4. *J. Asian Earth Sci.*, X(3), 100027. Doi: 10.1016/j.jaesx.2020.100027.
- Dung Chi Nguyen, et al., 2022. Precipitation response to Heinrich Event-3 in the northern Indochina as revealed in a high-resolution speleothem record. *J. Asian Earth Sci.*, X(7), 100090. Doi: 10.1016/j.jaesx.2020.100090.
- Ellwood B.B., T.H. Chrzanowski, F. Hroudá, G.J. Long, M.L. Buhl, 1988. Siderite formation in anoxic deep-sea sediments: A synergetic bacteria controlled process with important implications in paleomagnetism. *Geology*, 16(11), 980-982.
- Ellwood B.B., W.L. Gose, 2006. Heinrich H1 and 8,200 Year BP Climate Events Recorded in Hall's Cave, Texas. *Geology*, 34, 753-756.
- Ellwood B.B., F.B. Harrold, S.L. Benoist, P. Thacker, M. Otte, D. Bonjean, G.L. Long, A.M. Shahin, R.P. Hermann, F. Granjean, 2004. Magnetic susceptibility applied as an age-depth-climate relative dating technique using sediments from Scladina Cave, a late Pleistocene cave site in Belgium. *J. Archaeological Sci.*, 31, 283-293. Doi: 10.1016/j.jas.2003.08.009.
- Ellwood B.B., F.B. Harrold, S.L. Benoist, L.G. Straus, M. Gonzalez-Morales, K. Petruso, N.F. Bicho, Z.

- Zilhão, N. Soler, 2001. Paleoclimate and Intersite Correlations from Late Pleistocene/Holocene Cave Sites: Results from Southern Europe. *Geoarchaeology*, 16, 433-463.
- Ellwood B.B., K.M. Petruso, F.B. Harrold, J. Schuldenrein, 1997. High-Resolution Paleoclimatic Trends for the Holocene Identified Using Magnetic Susceptibility Data from Archaeological Excavations in Caves. *J. Archaeological Sci.*, 24, 569-573.
- Griffiths M.L., R.N. Drysdale, H.B. Vonhof, M.K. Gagan, J.-X. Zhao, L.K. Ayliffe, W.S. Hantoro, J.C. Hellstrom, I. Cartwright, S. Frisia, B.W. Suwargadi, 2010. Younger Dryas-Holocene temperature and rainfall history of southern Indonesia from $\delta^{18}\text{O}$ in speleothem calcite and fluid inclusions. *Earth Planetary Sci. Lett.*, 295, 30-36.
- Harrold F.B., B.B. Ellwood, P. Thacker, S. Benoist, 2004. Magnetic susceptibility analysis of sediments at the Middle-Upper Paleolithic transition for two cave sites in northern Spain. Zilhao, J.; D'Errico, F. (eds.) *The Chronology of the Aurignacian and of the Transitional Technocomplexes. Dating, Stratigraphies, Cultural Implications, Trabalhos de Arqueologia 33*. Lisboa, Instituto Português de Arqueologia, 301-310.
- Heinrich H., 1988. Origin and consequences of cyclic ice rafting in the northeast Atlantic Ocean during the past 130,000 years. *Quaternary Res.*, 29, 142-152.
- Hemming S.R., 2004. Heinrich events: Massive late Pleistocene detritus layers of the North Atlantic and their global impact. *Rev. Geophys.*, 42, RG1005, Doi: 10.1029/2003RG000128.
- Herz N., E.G. Garrison, 1998. *Geological Methods for Archaeology*. Oxford University Press, New York, 343p.
- Huong N.-V., Unkel I., Duong N.T., Thai N. Dinh, Do T.Q., Dang X.T., Nguyen T.H., Dinh X.T., Nguyen T. Anh N., Nguyen H.Q., Dao T.H., Nguyen T.H.T., Pham L.T.N., Le L.A., Vu V.H., A.E. Ojala, A. Schimmelmann, P. Sauer, 2023. Paleoenvironmental potential of lacustrine sediments in the Central Highlands of Vietnam: a review on the state of research. *Vietnam J. Earth Sci.*, 45(2), 164-182. <https://doi.org/10.15625/2615-9783/18281>.
- Keigwin L.D., J.P. Sachs, Y. Rosenthal, E.A. Boyle, 2005. The 8200 year B.P. event in the slope water system, western subpolar North Atlantic. *Paleoceanography*, 20, PA2003. Doi: 10.1029/2004PA001074.
- Laurin B. and D. D. Rousseau, 1985. Analyse multivariée des associations malacologiques d'Achenheim. Implications climatiques et environnementales. *Bulletin de l'Association française pour l'étude du Quaternaire*, 22(1), 21-30. <https://doi.org/10.3406/quate.1985.1523>.
- McManus J.F., R. Francols, J.M. Gherardl, L.D. Keigwin, S. Brown-Leger, 2004. Collapse and rapid resumption of Atlantic meridional circulation linked to deglacial climate changes. *Nature*, 428, 834-837.
- Moine O., D.D. Rousseau, D. Jolly, M. Vianey-Liaud, 2002. Paleoclimatic reconstruction using mutual climatic range on terrestrial mollusks. *Quaternary Res.*, 57(1), 162-172. <https://doi.org/10.1006/qres.2001.2286>.
- Morley M.W., P. Goldberg, 2017. Geoarchaeological research in the humid tropics: A global perspective. *J. Archaeological Sci.*, 77, 1-9. <https://doi.org/10.1016/j.jas.2016.11.002>.
- O'Connor S., A. Barham, K. Aplin, T. Maloney, 2017. Cave stratigraphies and cave breccias: Implications for sediment accumulation and removal models and interpreting the record of human occupation. *J. Archaeological Sci.*, 77, 143-159. <https://doi.org/10.1016/j.jas.2016.05.002>.
- Rasmussen S.O., K.K. Andersen, A.M. Svensson, J.P. Steffensen, B.M. Vinther, H.B. Clausen, M.-L. Siggaard-Andersen et al., 2006. A new Greenland ice core chronology for the last glacial termination. *J. Geophys. Res.*, 111, 1-16.
- Rohling E.J., H. Pälike, 2005. Centennial scale climate cooling with a sudden cold event around 8,200 years ago. *Nature*, 343, 975-979.
- Rohling E.J., Q.S. Liu, A.P. Roberts, J.D. Stanford, S. O. Rasmussen, P.L. Langen, M. Siddall, 2009. Controls on the East Asian monsoon during the last glacial cycle, based on comparison between Hulu Cave and polar ice-core records, *Quaternary Sci. Rev.*, 28, 3291-3302.
- Schmidt M.W., P. Chang, J.E. Hertzberg, B.L. Otto-Bliesner, 2012. Impact of abrupt deglacial climate

- change on tropical Atlantic subsurface temperatures. *Earth Atmos. Planet. Sci.*, 109(36), 14348-14352.
- Su Nguyen Khac, 2014. Report on Excavation Results at Con Moong Cave site (Thanh Hoa Province) in the years 2010-2014 (Documents Institute of Archeology, Hanoi).
- Su Nguyen Khac, 2009. Con Moong Cave: new data and new perceptions. *Vietnamese Archaeology*, 4, 43-54.
- Thompson L.G., E. Mosley-Thompson, M.E. Davis, P.N. Lin, K.A. Henderson, D.J. Cole, J.F. Bolzan, K.B. Liu, 1995. Late glacial stage and Holocene tropical ice core records from Huascarán, Peru. *Science*, 269, 46-50.
- Thong Pham Huy, 1980. Con Moong cave: A noteworthy archaeological discovery in Vietnam. *Asian Perspectives*, 23(1), 17-21.
- Walker M., S. Johnsen, S.O. Rasmussen, T. Popp, J.-P. Steffensen, P. Gibbard, W. Hoek, J. Lowe, J. Andrews, S. Björck, L.C. Cwynar, K. Hughen, P. Kershaw, B. Kromer, T. Litt, D.J. Lowe, T. Nakagawa, R. Newnham, J. Schwander, 2009. Formal definition and dating of the GSSP (Global Stratotype Section and Point) for the base of the Holocene using the Greenland NGRIP ice core, and selected auxiliary records. *J. Quaternary Sci.*, 24, 3-17.
- Walker M., S. Johnsen, S.O. Rasmussen, J.-P. Steffensen, T. Popp, P. Gibbard, W. Hoek, J. Lowe, J. T. Andrews, S. Björck, L. Cwynar, K. Hughen, P. Kershaw, B. Kromer, T. Litt, D.J. Lowe, T. Nakagawa, R. Newnham, J. Schwander, 2008. The Global Stratotype Section and Point (GSSP) for the base of the Holocene Series/Epoch (Quaternary System/Period) in the NGRIP ice core. *Episodes*, 31, 264-267.
- Wang Y.J., H. Cheng, R.L. Edwards, Z.S. An, J.Y. Wu, C.-C. Shen, J.A. Dorale, 2001. A high-resolution absolute-dated late Pleistocene monsoon record from Hulu Cave, China. *Science*, 294, 2345-2348.
- Wu B., N.Q. Wu, 2008. Paleoenvironmental study of S5 paleosol formation: Based on mollusk evidence. *Quaternary Sciences*, 28(5), 901-908 (in Chinese).
- Wu N.Q., T.S. Liu, X.P. Liu, Z.Y. Gu, 2002. Mollusk record of millennial climate variability in the Loess Plateau during the Last Glacial Maximum, Boreas, 31, 20-27.
- Wu N.Q., Y.P. Pei, H. Lu, Z. Guo, F. Li, T. Liu, 2006. Marked ecological shifts during 6.2-2.4 Ma revealed by a terrestrial molluscan record from the Chinese Red Clay Formation and implication for palaeoclimatic evolution. *Palaeogeogr., Palaeoclimatol. Palaeoecol.*, 233(3-4), 287-299. <https://doi.org/10.1016/j.palaeo.2005.10.006>.
- Wu N.Q., D.D. Rousseau, D.S. Liu, 1996. Land mollusk records from the Luochuan loess sequence and their paleoenvironmental significance, *Sci. China, Ser. D*, 39, 494-502.
- Wurster C.M., M.L. Bird, 2016. Barriers and bridges: Early human dispersals in equatorial SE Asia. Geological Society, London, Special Publications, 411(1), 235-250. <https://doi.org/10.1144/SP411.2>.